Studies of a polymeric chromium phosphinate. Electron-spin resonance and spin dynamics

P. D. Krasicky and R. H. Silsbee
Materials Science Center and the Laboratory of Atomic and Solid State Physics, Cornell University, Ithaca, New York 14853

J. C. Scott
IBM Research Center, San Jose, California 95193

(Received 7 August 1981; revised manuscript received 16 February 1982)

Magnetic properties of the chromium-tris-phosphinate polymer $\{Cr[O_2P(CH_3)(C_6H_5)]_2[O_2P(C_8H_{17})_2]\}_N$, known as PCrP-C, were studied with the use of conventional electron-spin-resonance (ESR) techniques. The chromium spins are coupled by antiferromagnetic Heisenberg exchange, with the value of $J/k_B=-2.5$ K for the nearest-neighbor exchange parameter determined from static magnetic susceptibility measurements. The ESR results show that the spins comprise a quasi-one-dimensional magnetic system with crystal-field anisotropy characterized by the site anisotropy parameter $|D|/k_B=0.21\pm0.02$ K. Magnetic interactions between linear polymer chain segments significantly influence the spin dynamics. A traditional memory function formalism is used to analyze the temperature-dependent ESR absorption line shape and linewidth. The theoretical predictions show general agreement with the experimental data, but certain discrepancies are obvious. In order to understand the underlying collective spin dynamics of exchange-coupled systems in a more intuitive, physical framework, three simple classical models were constructed: the two-spin model, the correlated cluster model, and the random-walk model. In addition to reproducing the results of the more formal, less transparent theory, these models also provide important insight into possible origins of the disagreement between the theory and experiments. Part of this disagreement, combined with the results of susceptibility measurements, strongly suggests that the chromium spin sites along PCrP-C chains are inequivalent with respect to the orientation of the principal axes of the crystal-field anisotropy. The remainder of the disagreement between the theory and data indicates that there are inherent inadequacies in the traditional theoretical approach.

I. INTRODUCTION

In a previous paper[1] (hereafter referred to as I) the structural and static magnetic properties of the semicrystalline chromium-tris-phosphinate polymer $\{Cr[O_2P(CH_3)(C_6H_5)]_2[O_2P(C_8H_{17})_2]\}_N$, abbreviated as PCrP-C, were reported. The present article extends that study to the dynamical aspects of the magnetism as probed by electron-spin resonance (ESR).

As discussed in detail in I, PCrP-C is a linear polymer with chain segments of length $\ell \geq 20$ times the nearest-neighbor chromium spacing $a=4.52$ Å. Samples were prepared in the form of sheets, such that chains tend to align locally parallel to one another with a higher probability of lying parallel to the sample plane than perpendicular to it. Nearest-neighbor antiferromagnetic exchange coupling along the chains is of the Heisenberg type $-2J\vec{s}_n\cdot\vec{s}_{n+1}$, with $J=-2.5$ K. The susceptibility data were interpreted in terms of an axial site anisotropy $Ds_{n||}^2$, where $s_{n||}$ is the spin component parallel to the chain length, and an easy-plane anisotropy with $D\lesssim 0.1$ K was implied. The question of whether or not there are deviations from this simple type of site anisotropy is addressed in Sec. IV, but for the moment possible complications will be ignored. Intrachain and interchain dipolar coupling, characterized by strengths of $g^2\mu_B^2/a^3=0.026$ K and $g^2\mu_B^2/b^3\simeq 0.005$ K, respectively, where $b=7.81$ Å is the smallest interchain spacing, are also present and contribute a portion to the apparent D. As will be shown in Sec. IV, the site anisotropy, as modulated by the antiferromagnetic exchange, is the primary homogeneous broadening mechanism for the ESR absorption in PCrP-C.

After a review in Sec. II of experimental ESR results, Sec. III deals with the theoretical description of spin dynamics. The existing formal theoretical treatments outlined in III, though powerful, are not intuitively transparent. To aid physical understanding, three simple classical models were constructed to cast the collective spin dynamics into a more intuitive framework.

A previous ESR study of a crystalline chromium phosphinate dimer known as DPACr, with a chemical structure fundamentally similar to that of PCrP-C, first suggested the formulation of the two-spin model.[2] The correlated cluster model evolved as a generalization of the two-spin model to describe chains of many coupled spins at low temperatures, while the high-temperature behavior required a somewhat different approach, embodied in the random-walk model. These three models are discussed in detail in Sec. III. Section IV is devoted to a summary of points of agreement and disagreement between theory and experiments, using the classical models to provide insight into possible sources of discrepancy.

II. EXPERIMENTAL RESULTS

ESR spectra of PCrP-C were taken at X band in the temperature range from 1.5 to 300 K for different sample orientations relative to the static magnetic field $\vec{H}$. Two samples taken from different batches of the material were examined. Temperature was controlled and monitored above 4 K by an Oxford DTC-2 temperature controller, while immersion in liquid helium was used in the range from 1.5 to 4 K.

Derivative spectra were recorded using conventional field modulation and phase-sensitive detection techniques. Typical spectra are shown in Fig. 1. At room temperature a single Lorentzian line is seen. The line is centered at $g=1.98$, the typical value for Cr(III) octahedrally coordinated to oxygens.[3–7] The Lorentzian shape is confirmed, as shown in Fig. 2, by the straight line obtained in a plot of $|(H-H_0)/I'|^{1/2}$ vs $(H-H_0)^2$, where I' is the derivative signal amplitude, H is the magnetic field strength, and H_0 is the field at the line center. The peak-to-peak derivative linewidth ΔH_{pp} is about 200 G, and is weakly anisotropic, with about a 15% increase as the field is rotated from perpendicular to the sample plane to parallel.

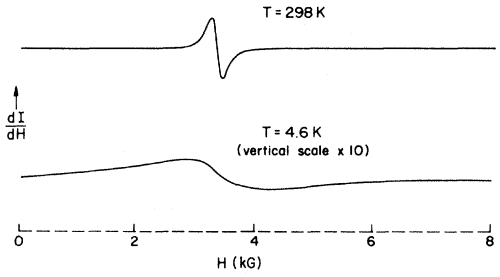

FIG. 1. Derivative of ESR absorption in PCrP-C, taken at a microwave frequency of 9.345 GHz.

As the temperature is lowered from room temperature, changes are observed in first the linewidth and then the line shape. Between $T=300$ K and $T=20$ K the line remains Lorentzian and centered at $g=1.98$, but variations in linewidth and total intensity occur. The line intensity, measured by the product of the amplitude and the square of the peak-to-peak derivative linewidth follows the temperatures variation of the static susceptibility, as expected according to the Kramers-Kronig relation,[8–11] within about 20%.

Below $T=20$ K, the line shape changes very noticeably. The line becomes asymmetric as shown in Fig. 1, and considerable intensity is shifted into a high-field tail beyond 12 kG, which represents the operating limit for the magnet used. The significance of these changes can be emphasized by once integrating the derivative spectrum taken at $T=3.6$ K to obtain the absorption profile shown in Fig. 3. As can be seen, there is substantial intensity in the high-field portion of the line as well as at zero field, and the asymmetry is more obvious. Because of the zero-field absorption, there is ambi-

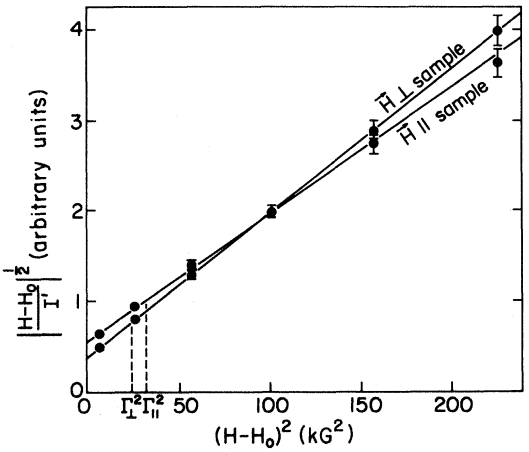

FIG. 2. Verification of Lorentzian ESR line shape in PCrP-C at $T=298$ K. H is the static magnetic field strength, H_0 is the field strength at the center of the line, I' is the derivative of ESR absorption. $\Gamma_\perp$ and $\Gamma_\parallel$ are the half-widths at half maximum.

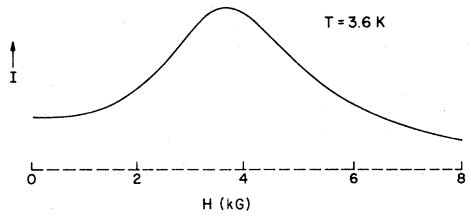

FIG. 3. Low-temperature ESR absorption in PCrP-C obtained by numerically integrating the derivative spectrum. The baseline cannot be determined from the measured derivative because of the continuing decrease in absorption at the upper field limit of 12 G.

guity in determining the baseline for the absorption profile, so it is difficult to measure the total intensity to better than a factor of 2.

The peak-to-peak derivative linewidth ΔH_{pp} is plotted as a function of temperature T in Fig. 4 for the different samples. The values shown represent appropriate averages of the values measured for $\vec{H}$ parallel and perpendicular to the sample plane. Although the data for the two samples show some differences, probably related to structural variations which influence site anisotropy and exchange, the essential features are the same and, as will be noted later, both sets of data show the same substantial discrepancies with the theory. The essential features, also observed in the ESR of other one-dimensional antiferromagnets such as TMMC $[(CH_3)_4\,NMnCl_3]$ (Ref. 12) and CMC $(CsMnCl_3 \cdot 2H_2O)$ (Ref. 13), are the minimum in ΔH_{pp} as a function of T and the monotonic rise

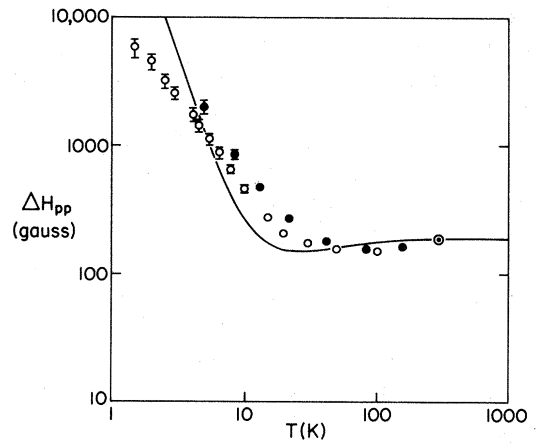

FIG. 4. Peak-to-peak derivative ESR linewidth in PCrP-C. The open and closed circles represent data for different samples, and the solid line is a calculation obtained from the memory function formalism described in Sec. III and fit to the high-temperature data.

with decreasing T at low temperatures, and are discussed in detail in Sec. IV. Additional details of the experiments, as well as measurements of linewidth anisotropy and the effect of polymer swelling, are available in I and Ref. 14.

III. COLLECTIVE SPIN DYNAMICS

A. Introduction

The dynamics of extended, exchange-coupled spin systems at low temperatures is usually described in terms of spin waves. Near $T=0$ where spin correlations extend over large distances, spin-wave excitations of small amplitude are propagating normal modes.[15–17] At higher temperatures the correlations become shorter in range, and only those spin waves whose wavelengths are appreciably shorter than the static correlation length persist as propagating modes. Those with wavelengths longer than the correlation length become overdamped modes. Finally, as the correlation length becomes comparable with the lattice constant, the dynamics of the system is more appropriately described by diffusion rather than propagation.[18,19]

In order to establish an intuitive framework within which the detailed dynamical behavior of such coupled spin systems can be understood on a physical basis, two simple classical models have been constructed. The first is the random-walk model which describes the high-temperature behavior in terms of spin fluctuations which diffuse through the system by a simple hopping process. The second is the correlated cluster model which for low temperatures treats the system as a collection of weakly interacting clusters of correlated spins, each cluster behaving as an independent dynamical entity. Since this model draws heavily upon ideas contained in the two-spin model for a classical dimer, a discussion of that model precedes the description of the correlated cluster model.

A more traditional and more rigorous procedure for calculating temperature-dependent dynamical properties of such systems has also been applied to the ESR in PCrP-C. This method focuses upon the relaxation function, or the dynamic spin-spin correlation function, and its associated memory function, and is summarized at the end of this section. Throughout this and all subsequent sections, for convenience, $\hbar$ and k_B will be taken equal to unity, and all energies and frequencies expressed in temperature units.

B. The random-walk (high-temperature) model

Exchange coupling and translational spin motion are known to have similar effects on the ESR of systems consisting of many spins on a lattice with random local magnetic fields at the lattice sites.[8,9,11,20,21] In the absence of exchange or translation the distribution of observed precession frequencies of the spins at the various sites directly reflects the distribution of local-field strengths. However, if the spins are free to wander through the lattice, they will sample different local fields at different times and the effects of the different field strengths will tend to be averaged out. If the motion is rapid enough, the distribution of observed precession rates will be substantially narrower than the distribution of local precession rates, and the ESR spectrum is said to be "motionally narrowed."

Similarly, if the spins are bound to the lattice sites but are coupled by sufficiently strong exchange interactions, an "exchange narrowing" will be observed. These interactions allow the spins to exchange fluctuations with one another. The fluctuations, in effect, wander about the lattice, and in this way different local fields are sampled. But the detailed physical description of the exchange narrowing process is somewhat more complicated than that for motional narrowing. To illustrate the dramatic consequences of dimensionality on this narrowing process in exchange-coupled spin systems at high temperatures, the spin dynamics will, for simplicity, be modeled in terms of diffusing spins rather than spin fluctuations.

Consider a regular lattice of unspecified dimensionality at whose sites there exist local fields of randomly distributed strengths but whose directions are parallel or antiparallel to a given axis. A spin at any site will precess at a rate ω_a determined by the strength of the local field and in a sense determined by the particular direction of that field. Let the distribution of the local precession frequencies of the spins be characterized by a width $\Delta\omega_a$. For instance, in a system with site anisotropy, $\Delta\omega_a \sim D$, the single-site anisotropy energy parameter.

Suppose now that the spins diffuse about from site to site on the lattice by a random-walk process in which each spin sits on a given lattice site only for a time t_e after which it hops in a random direction to one of the neighboring sites. In analogy to an exchange-coupled system like PCrP-C, $t_e \sim 1/|J|$, where J is the exchange parameter. If one follows any particular spin as it wanders through the lattice, its precession in the local fields also takes place in steps by a random-walk process. The rms precessional phase acquired by a spin during one visit to a site is $\phi_1 \sim \Delta\omega_a t_e$. It is important to note that if the spin later makes visits back to the same site, the phase acquired at the site during different visits accumulates coherently. However, the phases accumulated at different sites add incoherently, since the local precession frequencies are randomly distributed.

Consider a three-dimensional lattice such as the simple cubic. After a time t ($>> t_e$), the number of hops which any particular spin executes is $N_h = t/t_e$. From random-walk arguments, the diffusion length or rms displacement of the spins from their initial locations in terms of a number of lattice constants, is $r \sim N_h^{1/2} \sim (t/t_e)^{1/2}$. The number of sites "accessible" to a given spin in a time t shall be defined as the total number of sites contained within a sphere of radius r, namely $N_r = 4\pi r^3/3 \sim (t/t)_e^{3/2}$. The fraction of these accessible sites which any one spin can actually encounter in time t is $N_h/N_r \sim (t_e/t)^{1/2}$, and this becomes very *small* with time. Hence, the probability that a spin returns to a site which it has visited previously is small. (Actually, the probability of eventual return is about 0.3, but the important point is that return is not a recurrent event.[22]) So, after a time t the rms phase accumulated by a spin is

$$\phi(t) \sim N_h^{1/2} \phi_1 \sim \Delta\omega_a t_e^{1/2} t^{1/2} . \tag{1}$$

In the ESR for such a system, the observed width of the resonance line in terms of frequency is described by the inverse of a transverse relaxation time T_2 can be defined as the time required for an ensemble of spins initially in phase with one another to become effectively dephased by their precession in the random local-field torques, or simply the time required for the rms phase accumulation per spin to become on the order of unity. Setting $\phi(T_2) \sim 1$ for this system yields

$$\Delta\omega \sim \frac{1}{T_2} \sim \Delta\omega_a^2 t_e , \tag{2}$$

which, in analogy to an exchange-coupled system with single-site anisotropy, becomes the familiar $\Delta\omega \sim D^2/|J|$. It can also be shown that the line shape will be approximately Lorentzian with a cutoff at $\omega \sim \pm |J|$ (see Sec. IV).

For one-dimensional systems the situation is different. While after a time t on a linear chain the rms displacement per spin is still $r \sim (t/t_e)^{1/2}$, the

number of accessible sites for a spin is the number of sites contained in a length $2r$ of the chain, or $N_r = 2r \sim (t/t_e)^{1/2}$. Since $N_h > N_r$, the average number of times a particular spin visits each of the sites is $N_s \sim N_h/N_r \sim (t/t_e)^{1/2}$, which becomes very *large* with time. (Return is now a recurrent event.[22]) This is the essential difference between one- and three-dimensional diffusion. The average phase accumulated per spin site is now

$$\phi_s(t) = N_s \phi_1 \sim \Delta\omega_a t_e^{1/2} t^{1/2} ,$$

rather than simply ϕ_1, and the rms total phase per spin becomes

$$\phi(t) \sim N_r^{1/2} \phi_s \sim \Delta\omega_a t_e^{1/4} t^{3/4} . \tag{3}$$

Hence, the ESR linewidth is now

$$\Delta\omega \sim \frac{1}{T_2} \sim \Delta\omega_a^{4/3} t_e^{1/3} , \tag{4}$$

or in the analogy, $\sim D^{4/3}/|J|^{1/3}$, in marked contrast to the three-dimensional result. As can be shown by more rigorous methods, the line shape will no longer be Lorentzian.[12,19]

One other relevant system is an array of parallel one-dimensional chains which interact with one another through some three-dimensional type of spin coupling which is much weaker than the intrachain interactions. The direct magnetic dipolar interaction is one such interchain coupling mechanism and is important in PCrP-C. The dynamical effect of this type of interaction is that fluctuations can now be exchanged between spins on different chains.

Continuing the analogy with the spin-hopping picture, spins must now be allowed to transfer from chain to chain. Let a given spin remain on a particular chain only for a time $t_c >> t_e$) after which it hops in a random direction to one of the neighboring chains. The magnitude of t_c will be on the order of $1/j$, where j represents some effective interchain coupling energy.

The hopping process between chains is a two-dimensional random walk. In a time t the rms spin displacement perpendicular to the chains is $r_\perp \sim (t/t_c)^{1/2}$, while that parallel to the chains is still $r_{||} \sim (t/t_e)^{1/2}$. The number of accessible sites is the total number of sites contained in the volume defined by these dimensions, namely, $N_r \sim r_\perp^2 r_{||} \sim t^{3/2}/t_c t_e^{1/2}$. From the preceding discussion it is known that during one visit to a chain the number of distinct sites which a given spin actually encounters is $N_c \sim (t_c/t_e)^{1/2}$. In a time t ($>> t_c$) the number of chain hops which this spin makes is $N_{ch} = t/t_c$, and in this time it can be expected to encounter not many more than $N_{max} \sim N_{ch} N_c \sim t/(t_e t_c)^{1/2}$ distinct sites. The ratio $N_{max}/N_r \sim (t_c/t)^{1/2}$, which represents the fraction of the accessible sites which the spin can reasonably hope to encounter, becomes very small with time. So if the spin were to return to a chain which it had visited previously it would be unlikely to encounter any sites which it had seen during those previous visits to that chain, and precessional phase would accumulate incoherently from chain to chain. (The otherwise recurrent one-dimensional return process is now cut off by interchain hopping.)

The rms phase has accumulated by a spin during one chain visit is $\phi_c \sim \Delta\omega_a t_e^{1/4} t_c^{3/4}$, according to previous arguments. The rms total phase accumulated in a time t ($>> t_c$) is therefore

$$\phi(t) \sim N_{ch}^{1/2} \phi_c \sim \Delta\omega_a (t_e t_c)^{1/4} t^{1/2} , \tag{5}$$

since the contributions from different chains add incoherently. The ESR linewidth is now given by

$$\Delta\omega \sim \frac{1}{T_2} \sim \Delta\omega_a^2 (t_e t_c)^{1/2} , \tag{6}$$

which is proportional to $D^2/|Jj|^{1/2}$ in the analogy.

C. The two-spin model

Consider a system of two identical spins subject to equivalent axial site anisotropies and coupled by antiferromagnetic Heisenberg exchange. The Hamiltonian for this system is written

$$\mathcal{H}_{12} = -2J \vec{s}_1 \cdot \vec{s}_2 + D s_{1z}^2 + D s_{2z}^2 , \tag{7}$$

where $J < 0$. Considering the spins as classical entities with the geometric configuration shown in Fig. 5 and torques derivable from an energy of the form, $\mathcal{H}_{12}$ the dynamics of the system can be described in the following way. If $|J| >> |D|$ and the angle γ is not too close to zero, the two spins $\vec{s}_1$ and $\vec{s}_2$ precess rapidly about their sum $\vec{S}$ because of the relatively large exchange torques. The total spin $\vec{S}$ then precesses more slowly about the z axis due to the effective anisotropy torque which is the sum of the average of the individual torques felt by $\vec{s}_1$ and $\vec{s}_2$ during one complete revolution about $\vec{S}$. This effective anisotropy torque is derivable from the effective anisotropy energy for the total spin $\vec{S}$, which is similarly the sum of the individual anisotropy energies averaged over one revolution. It is straightforward to show that

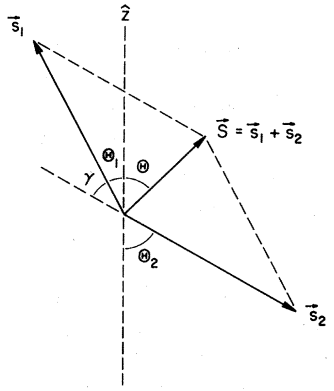

FIG. 5. Classical spin configuration for an exchange-coupled dimer with single-site anisotropy. The individual spins are denoted by $\vec{s}_1$ and $\vec{s}_2$, $\vec{S}$ is the total spin, and $\hat{z}$ is the anisotropy axis.

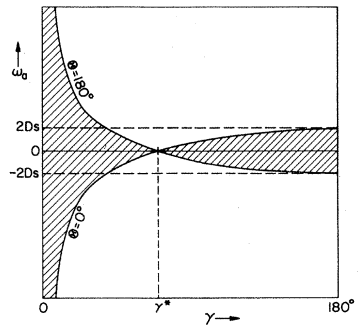

FIG. 6. Effective anisotropy precession frequency of the total classical dimer spin $\vec{S}$. γ is the angular deviation of the individual spins from antiparallel alignment, Θ is the angle between $\vec{S}$ and the anisotropy axis, and $\gamma^*=2\sin^{-1}\sqrt{(1/3)}=70.5°$. The shaded region corresponds to allowed values of ω_a.

this effective anisotropy energy has the form $D_S S_z^2$, where S_z is the z component of the total spin $\vec{S}$ and $D_S=\beta(\gamma)D$, with

$$\beta(\gamma)=\frac{3\sin^2(\gamma/2)-1}{4\sin^2(\gamma/2)} . \tag{8}$$

The factor $\beta(\gamma)$ is the classical analog of the conversion factors,

$$\beta_S=\frac{3S(S+1)-3-4s(s+1)}{(2S-1)(2S+3)} , \tag{9}$$

between single-site anisotropy parameters for individual quantum spins s and the effective parameters for the various multiplets of total quantum spin S, as computed by Owen.[23] States of large S in the quantum picture correspond to classical spin configurations with the spins nearly parallel and γ near 180°, while small S states correspond to the spins being nearly antiparallel and γ near zero. Since $S=2s\sin(\gamma/2)$, the classical conversion factor can be written as

$$\beta(\gamma)=\frac{3S^2-4s^2}{4S^2} , \tag{10}$$

which is precisely the form for β_S in the classical limit of large s and S.

The effective anisotropy torque on $\vec{S}$ is found to be

$$\begin{aligned}\tau_a &= 2D_S S^2\cos\Theta\sin\Theta \\ &= 2Ds^2[3\sin^2(\gamma/2)-1]\cos\Theta\sin\Theta . \end{aligned} \tag{11}$$

The precession frequency ω_a of $\vec{S}$ about the z axis is the ratio of the effective torque to the transverse moment $S_\perp=S\sin\Theta$, namely,

$$\omega_a=Ds\left[\frac{3\sin^2(\gamma/2)-1}{\sin(\gamma/2)}\right]\cos\Theta , \tag{12}$$

and is illustrated graphically in Fig. 6. For various angles Θ, the precession frequencies for different configuration angles γ lie within the envelope defined by the solid curves, which correspond to $\Theta=0°$ and 180°.

Notice that for small γ there is an apparent divergence in $\Delta\omega_a$, the spread in ω_a. However, if γ is small then the exchange torques are correspondingly reduced and the assumption of rapid exchange precession breaks down. The effects of exchange and anisotropy can no longer be decoupled from one another, and the system precesses in a coupled mode. From the preceding discussion, this coupling is expected when the anisotropy precession frequency ω_a becomes comparable to the exchange precession frequency $\omega_{12}=2Js\sin(\gamma/2)$. Using the small-$\gamma$ approximations $\omega_a\sim|D|s/\gamma$ and $\omega_{12}\sim|J|s\gamma$, one finds that if $\omega_a\sim\omega_{12}$, then $\omega_a\sim|JD|^{1/2}s$. The coupled mode which this frequency characterizes is analogous to the antiferromagnetic resonance (AFMR). In general, its dynamical description is complicated.[24,25] However, in the absence of an external magnetic field it can be easily shown that for $D<0$, the frequency of the AFMR is $\omega=\omega_{\rm AFMR}=|8JD|^{1/2}s$. In this case, each of the spins precesses about the z axis at a frequency $\omega_{\rm AFMR}$, but 180° out of phase with one another. With a static field $\vec{H}_0$ along the z axis the frequency becomes $\omega=\omega_{\rm AFMR}\pm\omega_0$, where $\omega_0=g\mu_B H_0$ is the Larmor frequency. For $\vec{H}_0$ in an arbitrary direction the analysis is quite involved, but, using effective field arguments,[24,25] it can be

shown that as long as $\omega_0 << \omega_{\mathrm{AFMR}}$, then for D of either sign, $\omega \sim \omega_{\mathrm{AFMR}} + O(\omega_0)$, in agreement with the previous estimate. Hence, when ω_a in the two-spin model becomes comparable to ω_{AFMR}, the divergence in $\Delta\omega_a$ is cutoff at $\Delta\omega_a \sim 2\omega_{\mathrm{AFMR}}$.

The important result, however, is that for spin configurations with γ near 0, the net magnetic moment S is very small since the spins are nearly antiparallel, while the individual anisotropy torques do not cancel but add. Hence, the precession frequency of the net moment is large. Such large precession frequencies would be expected primarily at low temperatures where in an ensemble of classical dimers there would be a high probability of configurations with γ near zero. The cutoff of the divergence in the precession frequencies, corresponding to the onset of the AFMR, occurs because at sufficiently low temperatures, the anisotropy tends to align the spins either along the z axis or in the plane perpendicular to it (depending on the sign of D), thereby limiting the magnitude of the anisotropy torques. At high temperatures most of the dimer pairs would be in configurations with γ appreciably different from zero and the spread in precession frequencies would be of the order of D.

As in the specific case of the AFMR, the presence of a static magnetic field $\vec{H}_0$, in general, complicates the spin dynamics in the two-spin model. In a manner analogous to that used for the AFMR, it can be shown that for an arbitrary direction of $\vec{H}_0$ relative to the z axis and for $\omega_0 << \omega_a$, the effect of this external field is essentially to shift the two-spin dimer precession frequency away from ω_a by an amount of the order of ω_0. Similarly, if $\omega_0 >> \omega_a$, then one can think of the anisotropy as shifting the precession frequency away from the free spin value ω_0 by an amount of the order of ω_a. Keeping this in mind, for simplicity in the ensuing discussion of ESR and spin dynamics the external magnetic field will not be considered explicitly.

In an antiferromagnetic quantum dimer (small s), the observation of large shifts in the ESR signal away from ω_0 is prohibited by the discrete energy spacing of the total spin-multiplet states. The multiplets with $S \neq 0$ are split by the anisotropy with effective anisotropy parameters of the order of magnitude of the single-site parameter D, since $|\beta_S|$ is of the order of unity for these multiplets. The resonances observed for these multiplets can be shifted from the Larmor frequency only by amounts of the order of D. In terms of the classical model these multiplets correspond to spin configurations with γ appreciably different from zero so that ω_a cannot be much larger than D. The $S=0$ multiplet corresponds to $\gamma=0$, but no resonance is possible because it is an isolated singlet. Hence, in such dimeric systems the AFMR mode with large frequency shifts is not observed because of quantum effects.

However, for a polymer such as PCrP-C, the ideas contained in the classical two-spin model do have significant bearing on the ESR problem. In the polymer at low temperatures, the spins $\vec{s}_1$ and $\vec{s}_2$ can be identified as the two nearly antiparallel sublattice magnetizations due to the spins which lie within a distance of the order of the static correlation length along a chain. Since the eigenstates of the polymer spin system are much more densely packed, there will be an appreciable density of states corresponding to sublattice spin configurations with small γ, and the classical description provides a useful model.

D. The correlated cluster (low-temperature) model

Consider a one-dimensional system of classical spins, each of magnitude s, which are located at equally-spaced sites on a linear chain. Let nearest-neighbor spins be coupled by an antiferromagnetic Heisenberg exchange interaction of the form $\mathscr{H}_{nn+1} = -2J\,\vec{s}_n \cdot \vec{s}_{n+1}$, where n refers to the site position along the chain, and $J<0$. Such interactions tend to align spins antiparallel to one another, but the effect will be negligible at temperatures high compared to $T_e \equiv 2|J|s^2$. As the temperature is lowered, spin-alignment correlations develop. The static correlation function $\langle \vec{s}_n \cdot \vec{s}_{n+1} \rangle$, where the brackets indicate a thermal average, can be easily computed as a function of temperature for such a system.[26] The result is

$$\langle \vec{s}_n \cdot \vec{s}_{n+1} \rangle = -s^2 u \ , \tag{13}$$

where $u = \coth x - x^{-1}$ and $x = T_e/T$. Notice that $\vec{s}_n \cdot \vec{s}_{n+1} = -s^2 \cos\theta_1$, where θ_1 is the angle by which the two successive spins deviate from antiparallel alignment. Hence $u = \langle \cos\theta_1 \rangle$ represents a measure of the thermal deviations of neighboring spins from such alignment. For $T << T_e$ or $x >> 1$, $u \simeq 1 - x^{-1}$ and θ_1 will always be close to zero. Using the approximation $\cos\theta_1 \simeq 1 - \theta_1^2/2$ the rms thermal value of θ_1 is found to be

$$\theta_{1\ \mathrm{rms}} \simeq \left[\frac{2}{x}\right]^{1/2} \sim \left[\frac{T}{T_e}\right]^{1/2} . \tag{14}$$

The correlation function $\langle \vec{s}_n \cdot \vec{s}_{n+m} \rangle$ is found to be

$$\langle \vec{s}_n \cdot \vec{s}_{n+m} \rangle = s^2(-u)^m , \tag{15}$$

which, by similar manipulation, yields

$$\theta_{m\ \mathrm{rms}} \simeq m^{1/2}\theta_{1\ \mathrm{rms}} \tag{16}$$

for the rms thermal deviation angle between spins m lattice sites apart when $T << T_e$. This result can also be obtained by simply realizing that as one progresses along the chain from site n to site $n+m$, the small thermal deviation angles between successive spins add in a random-walk fashion to give the net thermal angle between the spins on sites n and $n+m$, as the calculation indicates.

The essence of the correlated cluster model is the use of such random-walk arguments to obtain estimates to lowest order in T/T_e for rms values of various thermally excited quantities which describe the ensemble of classical spins just described. The basic physical idea is that at low temperatures ($T << T_e$), sufficient static correlations exist to regard a group of correlated spins as a dynamical unit or cluster. As long as $\theta_{m\ \mathrm{rms}} \lesssim 1$, the spins $\vec{s}_n$ and $\vec{s}_{n+m}$ are regarded as correlated. The correlation length, which corresponds to the size of a cluster, is defined as the number ξ of lattice constants along the chain required to make $\theta_{\xi\ \mathrm{rms}} \sim 1$. This yields

$$\xi \sim \frac{T_e}{T} , \tag{17}$$

a result which is alternatively obtained by setting $\ln(\langle \vec{s}_n \cdot \vec{s}_{n+\xi} \rangle / s^2) = -1$, subject to $x >> 1$.

To establish the connection with the PCrP-C problem, let there be a spin anisotropy energy of the form Ds_{nz}^2 at each site, where the z axis is simply the chain axis and $|D| << |J|$. The anisotropy will cause the correlated spin clusters to precess essentially as rigid units with neighboring spins nearly antiparallel. Its effects on the static spin correlations will for the moment be ignored.

In Fig. 7, the spins within a cluster are separated into antiparallel sublattices to illustrate the addition of the individual magnetic moments to give the sublattice moments $\vec{S}_1$ and $\vec{S}_2$, and the net cluster moment $\vec{S}$. The rms net thermally exicted moment S can be thought of as the incoherent sum of the rms moments of pairs of neighboring spins in the cluster. The rms pair moment is

$$s_{\mathrm{pair}} = 2s \sin\left(\frac{\theta_1}{2}\right) \simeq \theta s \sim \left(\frac{T}{T_e}\right)^{1/2} s ,$$

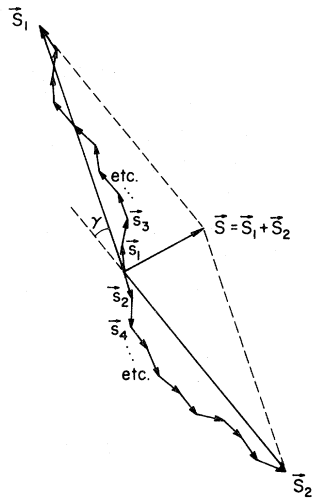

FIG. 7. Classical spin cluster configuration for a polymer, with individual spins $\vec{s}_i$ separated into sublattices. The total sublattice spins are denoted by $\vec{S}_1$ and $\vec{S}_2$.

so that the net moment per cluster is

$$S \sim \left(\frac{\xi}{2}\right)^{1/2} s_{\mathrm{pair}} \sim s . \tag{18}$$

S may alternatively be related to the magnitudes S_1 and S_2 of the sublattice moments and the thermally excited angle γ between them. The sublattice moments are

$$S_1 = S_2 = S_{\mathrm{sub}} \sim \left(\frac{\xi}{2}\right) s \sim \left(\frac{T_e}{T}\right) s ,$$

giving

$$S = 2S_{\mathrm{sub}} \sin\frac{\gamma}{2} \simeq S_{\mathrm{sub}}\gamma \sim \left(\frac{T_e}{T}\right)\gamma s . \tag{19}$$

Equating this expression to that in Eq. (18) yields an estimate for the rms value of γ, namely

$$\gamma \sim \frac{T}{T_e} . \tag{20}$$

The cluster configuration is defined by the rms values of the various thermally excited quantities. The dynamics of a cluster can be described in terms of the two-spin model which was discussed earlier in this section. The exchange torques within a cluster cause the two sublattices to precess about the net moment $\vec{S}$, while the anisotropy torques cause $\vec{S}$ to precess about the z axis. But a new feature is that clusters may interact with one

another through the exchange torques exerted between the spins at the arbitrarily defined boundaries between the clusters.

If γ is not too small then $\vec{S}_1$ and $\vec{S}_2$ will precess rapidly about $\vec{S}$ at a frequency given by

$$\omega_{\rm sub}\sim\frac{\tau_{\rm sub}}{S_{\rm sub}}\sim\frac{|J|s^2}{(\xi/2)s}\sim\frac{T}{s}\ , \tag{21}$$

where $\tau_{\rm sub}$, as shown in Appendix A, is simply the coherent sum of the ξ individual exchange torques, each of magnitude $|2J\vec{s}_n\times\vec{s}_{n+1}|\sim|J|s^2\gamma$, exerted by the spins of one sublattice on those of the other, or $\tau_{\rm sub}\sim\xi|J|s^2\gamma\sim|J|s^2$. If, on the other hand, γ becomes too small then the exchange torques no longer dominate but couple with the anisotropy torques to cause the spin system to precess in the zero wave-vector spin-wave mode, or antiferromagnetic resonance (AFMR),[24,25] whose frequency is $\omega_{\rm AFMR}=4|JD|^{1/2}s$. (The expression for $\omega_{\rm AFMR}$ for the polymer is greater by a factor of $\sqrt{2}$ than that for the dimer because each spin is exchange coupled to two neighbors in the polymer but only to one in the dimer.) This behavior occurs when $\omega_{\rm sub}\sim\omega_{\rm AFMR}$, or $T\sim T_a\equiv4|JD|^{1/2}s^2$. Therefore, for the present discussion the temperature must be restricted to the range $T>>T_a$.

Under the condition of rapid-exchange precession, the net cluster moment $\vec{S}$ will precess about the z axis due to the anisotropy torques at a frequency which, according to the two-spin model (Sec. II B), is

$$\omega_a=\frac{Ds[3\sin^2(\gamma/2)-1]\cos\Theta}{\sin(\gamma/2)}$$
$$\sim\left[\frac{T_e}{T}\right]D\cos\Theta\ . \tag{22}$$

Notice once more that $\Delta\omega_a$, the spread in ω_a, gets very large at low temperatures, because the net cluster moment remains constant and the anisotropy torque is proportional to the cluster size. The divergence is again cut off by the onset of AFMR at $T\sim T_a$.

In the correlated cluster model, however, the clusters interact through torques across their ends. These torques are nearest-neighbor exchange torques of the form $\vec{\tau}_e=-2J\vec{s}_n\times\vec{s}_{n+1}$. They are thermally activated, fluctuating, of magnitude $\tau_e\sim2|J|s^2\theta_1$, and have a correlation time $t_1\sim1/(|J|s)$, which roughly represents the time for an individual spin to precess about its mean orientation in response to the exchange torques from its neighbor. The influence of these fluctuating torques is to destroy the cluster configuration, but because they are rapidly fluctuating, their effects accumulate incoherently with time. In a time t_1, the net transverse change in one of the sublattice moments of a cluster due to these external torques is $\sim\tau_e t_1$, so that after a time t ($>>t_1$) the accumulated change is

$$\Delta S_{\rm sub}\sim\left[\frac{t}{t_1}\right]^{1/2}\tau_e t_1\sim\tau_e t_1{}^{1/2}t^{1/2}\ .$$

The cluster correlation time t_e is defined as the time required for $\Delta S_{\rm sub}$ to become $\sim S$, the rms net thermally activated cluster moment, yielding

$$t_e\sim\left[\frac{T_e}{T}\right]\frac{1}{|J|s}\sim\frac{s}{T}\ . \tag{23}$$

Therefore, the sublattice moments $\vec{S}_1$ and $\vec{S}_2$, which precess about $\vec{S}$ at a rate $\omega_{\rm sub}\sim T/s$, will on the average complete some reasonable fraction of one revolution before the cluster configuration is destroyed by interactions with neighboring clusters. The net effective anisotropy torque on a cluster is, therefore, roughly the sum of the anisotropy torques on the individual spins in the cluster averaged over a revolution.

The precession of a cluster due to the anisotropy torques takes place in a random-walk fashion since the cluster configuration fluctuates on a time scale t_e. As long as $\Delta\omega_a t_e<<1$, the ESR observed in such a system is simply an exchange-narrowed cluster resonance, and using $\Delta\omega_a\sim(T_e/T)Ds$, the absorption linewidth is given by

$$\Delta\omega\sim\Delta\omega^2 t_e\sim\left[\frac{T_e}{T}\right]^3\frac{D^2}{|J|}s\ . \tag{24}$$

The T^3 divergence at low temperatures is due to the constant net cluster moment, the increasing anisotropy torque as the cluster size increases, and the decreasing effectiveness of the exchange narrowing by coupling to neighboring clusters. The results are valid only in the regime $\Delta\omega_a t_e<<1$ or $T>>|JD|^{1/2}s^2$. The regime $T<4|JD|^{1/2}s^2$ is also that in which the anisotropy aligns the spins[27] and in which quantum properties of the system are expected to become evident. Although the applicability of the correlated cluster model as it stands does not extend into this lower temperature range, the physical ideas contained in this simple picture elucidate the important features of the dynamical behavior of such exchange-coupled systems and provide useful suggestions for methods by which to approach the lower temperature problem. In par-

ticular, the model serves as a useful framework for speculations as to the physical basis of deviations of observed behavior from that predicted by a more rigorous theories.

E. Formalism

1. Outline

The traditional method for describing in more rigorous terms the ESR of systems with large numbers of exchange-coupled spins utilizes a memory function formalism involving spin and torque correlation functions. The details of this method are described elsewhere.[8,11,12,28–35] The application of the method to the ESR in PCrP-C is outlined briefly here, with notation following that set forth in Ref. 12.

The exchange and Zeeman Hamiltonians, are, respectively,

$$\mathscr{H}_e=-2J\sum_n \vec{s}_n\cdot\vec{s}_{n+1}\ , \tag{25}$$

$$\mathscr{H}_z=g\mu_B H\sum_n s_{nz}\ , \tag{26}$$

where the static magnetic field $\vec{H}$ is along the z axis and n is the site location index. The local-field line broadening interaction for PCrP-C is single-site anisotropy written as

$$\mathscr{H}'=D\sum_n s_{n||}^2\ , \tag{27}$$

where $||$ refers to the chain-length direction. After considerable algebra the resulting ESR line-shape profile is given by

$$I(\Omega)=\frac{1}{\pi}\frac{\psi_1(\Omega)}{[\Omega-\psi_2(\Omega)]^2+[\psi_1(\Omega)]^2}\ , \tag{28}$$

where $\Omega=\omega-\omega_0$,

$$\psi_1(\Omega)=\int_0^\infty \psi(t)\cos\Omega t\,dt\ , \tag{29a}$$

$$\psi_2(\Omega)=\int_0^\infty \psi(t)\sin\Omega t\,dt\ , \tag{29b}$$

and the torque correlation function $\psi(t)$ has the form $\psi(t)=\psi_s(t)+\psi_d(t)$, describing, respectively, the short- and long-time behaviors of the decay of the local-field torques. The forms of these functions are as follows:

$$\psi_s(t)=M_2 e^{(-1/2)\omega_e^2 t^2}\ , \tag{30}$$

$$\psi_d(t)=\sum_{m=0}^{2}\psi_{dm}(t)\ , \tag{31}$$

$$\psi_{dm}(t)=A_m F_n^2(\eta)h(T)t^{-1/2}e^{-\omega_c t}\cos m\omega_0 t\ . \tag{32}$$

The second moment M_2 and correlation frequency ω_e are given by

$$M_2=\tfrac{2}{5}D^2 s^2(1+\cos^2\eta)f(T)\ , \tag{33}$$

$$\omega_e=2|J|s\left[\frac{g(T)}{f(T)}\right]^{1/2}\ , \tag{34}$$

while the other quantities are specified by the following relations:

$$A_0=0.8B,\ A_1=2B,\ A_2=0.2B\ ,$$

$$B=0.169D^2 s_c^{3/2}|2J|^{1/2}\ ,$$

$$F_0(\eta)=\tfrac{3}{2}(\cos^2\eta-\tfrac{1}{2})\ ,$$

$$F_1(\eta)=\sin\eta\cos\eta\ ,$$

$$F_2(\eta)=\sin^2\eta\ ,$$

$$f(T)=\left[\frac{1+u}{1-u}\right]\left[\frac{1+v}{1-v}\right]\ , \tag{35a}$$

$$g(T)=3\left[\frac{1+u}{1-u}\right]\left[\frac{u+v}{x}\right]\ , \tag{35b}$$

$$h(T)=\left[\frac{1-u}{1+u}\right]^{1/2}\left[\frac{1+v}{1-v}-\frac{2u}{1-u^2}\right]\ , \tag{35c}$$

$$u=\coth x-x^{-1},\ v=1-3ux^{-1}\ ,$$

$$x=T_e/T,\ T_e=2|J|s_c^2\ ,$$

where η is the angle between $\vec{H}$ and the chain axis, $s_c=[s(s+1)]^{1/2}$, and the torque correlation cutoff frequency is $\omega_c=\omega_i+\Delta\Omega$, ω_i describing the strength of additional interactions (not included in $\mathscr{H}'$) responsible for cutting off the otherwise slow decay of $\psi_d(t)$, and $\Delta\Omega$ being a measure of the linewidth determined self-consistently from Eq. (28).

Some further simplifications are possible for PCrP-C. The small angular anisotropy observed (only $\sim 15\%$ of the linewidth itself) indicates that most of the angular dependence has been washed out by disorder in chain packing. For simplicity, the angular factors involving η are averaged over an isotropic distribution of chain orientations. The observation of a Lorentzian line shape implies that the integral transforms simplify to

$$\psi_1(\Omega)\simeq\int_0^\infty \psi(t)dt\equiv\Gamma\ , \tag{36a}$$

$$\psi_2(\Omega)\simeq 0\ . \tag{36b}$$

This, as expected, reduces the line-shape profile to

$$I(\Omega)=\frac{1}{\pi}\frac{\Gamma}{\Omega^2+\Gamma^2} \tag{37}$$

and the half-width $\Delta\Omega$ at half maximum is seen to be Γ.

The Lorentzian shape also indicates that the additional cutoff interactions are more important than the self-consistent mechanism involving $\mathscr{H}'$ itself. From the fact that the Lorentzian shape extends out to at least 600 G on each side of the line center (see Fig. 2), the strength of the additional cutoff interactions can be estimated to be $\omega_i \gtrsim 0.07$ K. Specific mechanisms for this interaction are discussed in Sec. IV. The resulting peak-to-peak linewidth $\Delta H_{pp}(T)$ in the derivative of ESR absorption is now easily computed using $\Delta H_{pp}=(2/\sqrt{3})\Gamma/g\mu_B$.

2. *Comparison with the classical models*

It is appropriate to pause here to demonstrate the consistency of the results of the formal calculation with the predictions of the classical models presented in Sec. III. As long as $\omega_i << \omega_0 << |J|$, at high temperatures where $f(T)$, $g(T)$, and $h(T)$ are all $\simeq 1$, the largest contribution to the linewidth $\Delta\Omega$ comes from the term $\psi_{d0}(t)$ in the torque correlation function. This yields $\Delta\Omega \sim D^2/|J\omega_c|^{1/2}$. If the additional cutoff interaction were absent, then $\omega_c \sim \Delta\Omega \sim D^2/|J\Delta\Omega|^{1/2}$, which is solved for $\Delta\Omega$ to give $\Delta\Omega \sim D^{4/3}/|J|^{1/3}$. With an additional cutoff interaction such that ω_i is greater than the self-consistently determined linewidth, one has $\omega_c \sim \omega_i$, which yields $\Delta\Omega \sim D^2/|J\omega_i|^{1/2}$. On the other hand, in a three-dimensional system it can be shown that the asymptotic behavior of $\psi_d(t)$ is $\sim t^{-3/2}$, which makes the dominant contribution to the linewidth come from $\psi_s(t)$, namely $\Delta\Omega \sim D^2/|J|$. These results all agree with those predicted by the classical models. In general, it turns out that the evaluation of $\Gamma=\int_0^\infty \psi(t)dt$ is equivalent to determining the mean number of times a spin visits any particular site during the random-walk-hopping diffusion process. The significant contribution from the long-time tail of $\psi_d(t)$ for one-dimensional systems indicates that return visits are recurrent. In three-dimensions, the absence of any significant tail means that return visits are not recurrent.

At low temperatures $\psi(t)$ is dominated by $\psi_s(t)$, and the spin dynamics are no longer describable in terms of simple diffusion. Using the limiting forms for the temperature-dependent functions for small T (hence, large x), namely

$$f(T)\simeq\tfrac{4}{3}x^2\,, \tag{38a}$$

$$g(T)\simeq 12+O\left[\frac{1}{x}\right], \tag{38b}$$

one finds that

$$M_2\simeq\tfrac{32}{45}D^2s_c^2x^2\sim\left[\frac{T_e}{T}\right]^2 D^2\,, \tag{39}$$

$$\omega_e\sim 12\,|J|\,s_c/x\sim T\,. \tag{40}$$

The Lorentzian center of the line is now characterized by a half-width

$$\Delta\Omega\simeq\Gamma_s=\left[\frac{\pi}{2}\right]^{1/2}\frac{M_2}{\omega_e}\sim\left[\frac{T_e}{T}\right]^3\frac{D^2}{|J|}\,, \tag{41}$$

which is also predicted by the correlated cluster model [Eq. (24)]. Thus, the correlated cluster and random-walk models correctly represent the fundamental physics embodied in the more formal mathematical description of the spin dynamics.

IV. COMPARISON OF THEORY AND EXPERIMENT

A. A survey of the data

The temperature-dependent peak-to-peak linewidth $\Delta H_{pp}(T)$ in the derivative of the ESR absorption has been calculated, and the result is shown in Fig. 4 along with the experimental data. Using the parameter values $|J|=2.5$ K, $\omega_0=4.2$ K, and $\omega_i=0.07$ K, the value of D was adjusted so the calculation fit the data at the highest temperature, yielding $D=0.21\pm0.02$ K. This value is substantially larger than the value of $\lesssim 0.1$ K obtained from the susceptibility measurements, but comparable to that measured for the dimer ($D\sim 0.3$ K)[2] and for a monomeric form ($D\sim 0.4$ K).[36] The discrepancy is discussed later in this section.

Although the general contour of the calculated $\Delta H_{pp}(T)$ curve resembles that of the data, two discrepancies are obvious. First, the minimum in the theoretical curve in the intermediate temperature range (10 K $< T <$ 100 K) does not match that of the data. Second, the rate of change of the experimental linewidth at low temperatures ($T<10$ K) is considerably slower than that predicted by the theory. Whereas the theoretical linewidth

varies as T^{-3} at low temperatures, the experimental data reflect a behavior more like $T^{-1.5}$, although the dependence does not appear to be strictly a power law.

A similar theoretical analysis has been applied to the ESR in the one-dimensional antiferromagnets TMMC and CMC.[12,13] There the local magnetic fields responsible for the line broadening are due to intrachain dipolar coupling rather than site anisotropy. The difference arises because the orbital manifold for the electronic ground state of Cr^{+3} in PCrP-C is a septet split by the crystal field, while that of Mn^{+2} in the other materials is a singlet. Although there are some differences in the details of the calculations and the resulting temperature-dependent functions, the $\Delta H_{pp}(T)$ curve obtained from dipolar coupling has the same qualitative features as that based on site anisotropy. These features include the asymptotic approach to a constant value at high temperatures, the intermediate temperature minimum, and the T^{-3} divergence at low temperature. Because of this strong similarity, the effects of site anisotropy and dipolar coupling are virtually indistinguishable in experimental observations.

The results of the linewidth calculation based on the intrachain dipolar interaction can be applied to PCrP-C to furnish some idea of the relative importance of dipolar coupling and site anisotropy. If the linewidth in PCrP-C were due entirely to intrachain dipolar coupling, the value for the nearest-neighbor dipolar constant required to fit the theoretical $\Delta H_{pp}(T)$ to the observed linewidth at room temperature would be 0.050 ± 0.002 K. The actual value, based on the measured Cr-Cr nearest-neighbor spacing of $a=4.52$ Å, is $g^2\mu_B^2/a^3 = 0.026$ K. At high temperatures, where the contributions to the linewidth from dipolar coupling and site anisotropy are expected to add incoherently, the dipolar coupling is therefore responsible for only about one-fourth of the observed linewidth in PCrP-C, and a very substantial contribution must come from site anisotropy. By properly accounting for the dipolar interaction in PCrP-C, these calculations and the effective anisotropy parameter $D=0.21$ K previously determined from the linewidth data imply a value $D_a=0.18\pm0.02$ K for the parameter characterizing the single-site anisotropy alone. Note, however, that including the effects of intrachain dipolar coupling does not improve the overall agreement between the data and the theory because of the strong similarities in the temperature dependence of the linewidths from the two different interactions. Thus, other sources for the discrepancies must be considered.

At this point it is useful to consider specific mechanisms for the additional cutoff of the long-time decay of $\psi(t)$. One possibility is interchain magnetic dipolar coupling described by

$$\mathcal{H}_d=\sum_n\sum_{n'} g^2\mu_B^2[3(\vec{s}_n\cdot\hat{r}_{nn'})(\vec{s}_n\cdot\hat{r}_{nn'}) - \vec{s}_n\cdot\vec{s}_{n'}]/r_{nn'}^3 , \tag{42}$$

where n and n' refer to spin sites and $r_{nn'}$ is the distance between them. Explicit calculation of the dynamic correlation function for the dipolar torques,[12] which are modulated by intrachain exchange, shows that the effective strength j_d of the interchain dipolar interaction between any spin n on a given chain and all the spins on all parallel neighboring chains is given at high temperatures by

$$j_d \sim J_d^{4/3}/|J|^{1/3} , \tag{43}$$

where

$$J_d=\left[\sum_{\text{chains}} J_{d\ \text{chain}}^2\right]^{1/2} ,$$

and

$$J_{d\ \text{chain}}=g^4\mu_B^4 s^2(s+1)^2\sum_{n'}\sum_{n}\frac{f(nn')f(nn'')}{r_{nn'}^3 r_{nn''}^3} . \tag{44}$$

Here $f(nn'')$ is a function of the angle between the external magnetic field and the direction of separation between sites n and n', and the sums extend over all sites n' and n'' on one particular neighboring chain. For simplicity, the angular dependences are neglected and $f(nn')$ and $f(nn'')$ replaced by unity since only a rough estimate of the effective cutoff is needed. Hence,

$$J_{d\ \text{chain}}\sim g^2\mu_B^2 s^2\sum_{n'} r_{nn'}^{-3} .$$

These results can also be obtained by arguments of the random-walk model, as outlined in Appendix B.

The computation of $J_{d\ \text{chain}}$ is straightforward. Using the intrachain and interchain spacings $a=4.52$ Å and $b=7.81$ Å, respectively, J_d can be estimated by assuming four nearest-neighbor ($b=7.81$ Å) chains and neglecting the contributions from chains further away ($b\gtrsim 12.6$ Å), which can be shown to be insignificant within the accuracy of

this rough calculation. This gives $J_d \sim 0.12$ K, and $j_d \sim 0.04$ K. As pointed out in Appendix B, the corresponding cutoff frequency ω_i is a mean precession frequency of a spin subject to this interaction, or $\omega_i \sim j_d/s_c \sim 0.02$ K, to be compared with the estimate made earlier, $\omega_i \gtrsim 0.07$ K based upon the Lorentzian character of the line shape.

Another possible cutoff mechanism is chain branching. In a branched chain material, spins would diffuse one-dimensionally only over time scales for which the corresponding diffusion length $r(t)=(2Kt)^{1/2}$ is less than the distance ℓ between branch points. After that, the diffusion would proceed more rapidly, cutting off the slow one-dimensional decay of the torque calculations. The cutoff time t_b can be estimated by setting $r(t_b) \sim \ell$, which yields $t_b \sim \ell^2/2K$ and an effective cutoff strength $\omega_i \sim 1/t_b \sim K/\ell \sim 0.06$ K, using the lower bound $\ell = 20$ determined from the x-ray diffraction patterns. Based on these rough estimates it is possible that chain branching and interchain dipolar coupling could together account for the cutoff strength implied by the Lorentzian line shape. However, a more detailed examination of the cutoff process would be required to completely resolve the question. This will not be pursued here.

B. The intermediate temperature regime

One might wonder whether the agreement between the data and the theory could be improved with a different choice of parameter values in the calculation of $\Delta H_{pp}(T)$. It turns out that the minimum in the theoretical curve can be moved to a higher temperature by using a larger ω_i, giving less proportional weight to the diffusive contribution to the linewidth, and readjusting D to maintain the high-temperature fit. But unrealistically large values of ω_i are required to produce any noticeable change in the curve, and the low-temperature discrepancy still remains. Hence, the agreement cannot be improved simply by redefining parameter values.

The interchain dipolar interaction can itself make a contribution to the linewidth in addition to providing a cutoff mechanism. Incorporating the information from the preceding section concerning the chain packing arrangement in PcrP-C into the dipolar linewidth calculation[12] mentioned earlier, one can estimate an upper bound of only about 20 G for the contribution to the high-temperature linewidth from interchain dipolar coupling. Although the temperature dependence of this contribution may be somewhat different from that associated with the portions due to crystal-field anisotropy and intrachain dipolar coupling, the resulting deviation in the total linewidth from the dependence calculated previously is probably too small to observe.

It should be pointed out that discrepancies between experimental and theoretical temperature-dependent linewidths similar to those in PCrP-C also occur[12,13] for CMC and TMMC. Thus, while each material is expected to have its own distinctive properties, they all display certain common behavior which appears to be characteristic of one-dimensional Heisenberg antiferromagnets. Disagreement between the theory and experiments regarding these common traits seems to suggest a general inadequacy in the theory. This question is briefly addressed in Sec. V.

A possible source for at least some of the discrepancy between the predicted and observed linewidth variation in the intermediate temperature range lies in the procedure used to evaluate the long-time portion $\psi_d(t)$ of the torque correlation function under the condition of spin diffusion. The assumption is traditionally made that Fourier components with wave number q appreciably different from zero decay so rapidly in time that their effects can be neglected. It turns out that the temperature dependence of contributions to the linewidth from these higher q modes is rather different from that due to the modes with q near zero. In fact, modes with q near π begin to soften and persist as the temperature is lowered towards T_e and static correlations develop. In effect, the dynamics of these modes changes character so that a description in terms of simple diffusion is no longer adequate. The persistence of these modes tends to broaden the ESR, and by properly accounting for these effects the agreement between the theory and that data might be improved.

It should also be kept in mind that the rms strength of the interchain dipolar interaction is influenced by static spin correlations. Therefore, the effectiveness of this interaction as a mechanism for the cutoff of the slow one-dimensional diffusive decay of torque correlations is likely to be temperature dependent. The resulting effect on the ESR linewidth should be most apparent in the temperature range where static correlations are developing and where the diffusive contributions to the linewidths still dominate. This corresponds to T in the vicinity of T_e, which for PCrP-C is about 20

K. Since the exchange interaction is antiferromagnetic, the induced antiparallel spin alignment would tend to reduce the net effective dipolar coupling between any particular spin on one chain and the entire set of spins on a neighboring chain. The cutoff strength would thereby be reduced, resulting in an increased linewidth and a shift in the minimum in $\Delta H_{pp}(T)$ vs T to higher T.

C. The low-temperature regime

In the low-temperature range ($T<10$ K) the disagreement between the linewidth data and the theory is more dramatic. The theory predicts a T^{-3} dependence for $\Delta H_{pp}(T)$ in this range, whereas the data behave more like $T^{-1.5}$ for 3 K $<T<10$ K and deviate towards an even slower variation for $T<3$ K. As shown in Sec. III, the correlated cluster model provides an accurate physical description of the low-temperature classical spin dynamics and should help elucidate the source of these discrepancies.

In terms of the correlated cluster model, the T^{-3} divergence in $\Delta H_{pp}(T)$ for $T<<T_d$, is expected for the following reasons. As the temperature is lowered, the net thermally activated rms magnetic moment of a correlated spin cluster is independent of temperature, the net effective anisotropy torque is proportional to the cluster size $\xi\sim T_e/T$, and the fluctuating intercluster exchange interactions become less effective by another factor of T/T_e in narrowing the resonance line. However, near a temperature $T_a\equiv 4|JD|^{1/2}s_c^2$, the anisotropy begins to align spins relative to the anisotropy axis. When this occurs, spin-correlation functions used in the formal theory must be calculated with explicit account of $\mathscr{H}'$ taken in the thermal averaging process.[27] In terms of the correlated cluster model, the spin alignment relative to the anisotropy axis now restricts the range of polar angles relative to this axis which are available to the spins and prevents the net rms anisotropy torque from increasing as rapidly as expected in the absence of this alignment. Consequently, the T^{-3} divergence is softened for $T\lesssim T_a$, and the theoretical calculation of $\Delta H_{pp}(T)$ based on isotropic correlations due to exchange alone is, therefore, strictly valid only for $T>>T_a$.

When appreciable anisotropy alignment has taken place, the spin dynamics are then appropriately described in terms of spin waves. In particular, the observed ESR corresponds to the antiferromagnetic resonance (AFMR), which is a $q=0$ spin wave with a resonant frequency shifted away from the Larmor freuqency ω_0 by an amount of approximately $\omega_{\mathrm{AFMR}}=4|JD|^{1/2}s_c$, with some variation depending on the orientation of the static magnetic field relative to the anisotropy axis.[24,25] Because of this anisotropy in spin correlations and the onset of the AFMR, the increasing spread $\Delta\omega_a$ in the spin cluster precession frequencies as the temperature is lowered begins to be cut off at roughly ω_{AFMR} when $T\simeq T_a$. For $T\lesssim T_a$, $\Delta\omega_a$ and M_2 would approach the constant values $\Delta\omega_a\sim|JD|^{1/2}s_c$ and $M_2\sim\Delta\omega_a^2$, and the exchange would no longer provide any significant narrowing since $\omega_e\sim T/s_c$ which is $\lesssim\Delta\omega_a$. Thus, the observed spread in ESR frequencies should remain roughly constant, the T^{-3} divergence having been removed completely. However, the line-shape profile would no longer be a simple Lorentzian. Rather, one would expect a pair of AFMR lines, one on each side of $\omega=\omega_0$, to develop. (In a conventional ESR experiment where the magnetic field is swept with the frequency constant, the AFMR would appear at a field H shifted upwards from $g=2$ by roughly $\omega_{\mathrm{AFMR}}/g\mu_B$.)

From this discussion, it is apparent that there will be only a range of temperatures $T_a\lesssim T\lesssim T_e$ for which the linewidth can vary as T^{-3}. The values of these limits for PCrP-C calculated using $D=0.21$ K and $|J|=2.5$ K, are $T_a=11$ K and $T_e=19$ K. It is likely that such a range is too narrow for the T^{-3} dependence to develop, and only a transitory type of behavior can be observed. An analysis of the details of this transition, however, would require the numerical calculation of correlation functions and line-shape profiles with explicit account taken of the anisotropy alignment.[27]

Another more exotic possibility for the source of the low-temperature discrepancy between the ESR linewidth data and the calculation has been suggested by susceptiblity measurements made on PCrP-C. While the susceptibility is not as sensitive to the value of the effective anisotropy parameter D as is the ESR, the low-temperature static susceptibility anisotropy can be used to at least estimate D with an accuracy of about 30%. At $T=1$ K, the value deduced for the effective D is about 0.02 K, while at $T=6$ K the value is about 0.1 K. The ESR data suggests a value of about 0.21 K. Such an apparent temperature dependence for the measured D could be due to Cr site inequivalence along the PCrP-C chains. If the mag-

nitude of the single-site anisotropy and the orientation of its principal axes were different at different sites, then high-temperature measurements ($T >> T_e$) would yield a value for D which represents an rms average of the anisotropy strengths at the different sites, independent of principal axis orientations. However, at lower temperatures ($T \lesssim T_e$) where the exchange produces appreciable spin correlations, the measured D would characterize the collective anisotropy energy per spin within a correlated spin cluster and, therefore, represent a linear average of the directional variation of individual anisotropy energies for all the spins in a cluster. If the principal anisotropy axes were sufficiently different in orientation for different sites, then significant cancellation could occur in the linear averaging process, and the measured D at low temperatures would be considerably smaller than the single-site D, which the high-temperature data more accurately reflect. Since it is the effective D per spin for a correlated spin cluster which determines the cluster anisotropy torque, and hence, the ESR linewidth, and since the linewidth depends quadratically on this effective D, the rate of linewidth variation with temperature at low temperature could be softened quite dramatically, as observed, by orientational site inequivalence.

In addition, the onset of anisotropy alignment and the AFMR mode as the temperature is lowered would be suppressed by this disorder in the anisotropy. Comparison of the total integrated ESR intensities for PCrP-C at $T=300$ K and $T=4.5$ K with measured static susceptibilities at those temperatures show that much of the intensity expected on the basis of the Kramers-Kronig relation[8-11] appears to remain near $g=2$ down to at least approximately $T=4.5$ K. Although the AFMR cannot be observed directly because it occurs at a magnetic field strength beyond the range of the available experimental equipment, the intensity measurements do suggest that the AFMR is not setting in as quickly as one would expect for a system with equivalent spin sites.

Site inequivalence is indeed consistent with the molecular structure of the PCrP-C chains. Since the phosphinate bridges between neighboring chromiums differ in their organic side groups (two contain one each of methyl and phenyl, and the other has two octyls), one expects the otherwise trigonal symmetry at the Cr sites to be broken by the different electrostatic interactions or, more importantly, by bond distortions arising from differences in the morphology of these side groups.[37-40] While a detailed x-ray diffraction examination might detect such distortions, it is not likely that any useful quantitative estimate of their effects on the site anisotropy could be made.

Other factors which can influence the low-temperature spin correlations are the external magnetic field, finite chain lengths, and the quantum nature of the spins. However, simple arguments can be given to show that effects due to these factors should not be significant until $T < T_a$, where the effects of anisotropy alignment have already become apparent.[25,41,42]

V. COMMENTS AND CONCLUSIONS

The chromium phosphinate polymer PCrP-C is a member of a growing class of materials containing exchange-coupled metallic ions with one-dimensional collective magnetic properties. The present investigation, along with I, has demonstrated that PCrP-C exhibits magnetic behavior which is common to one-dimensional Heisenberg antiferromagnets such as TMMC and CMC.[12,13] This behavior includes the qualitative temperature dependence of the ESR and of the static magnetic susceptibility. The results of this study confirm the fundamentally one-dimensional character of the coupled spin system in PCrP-C, which is expected on the basis of the polymer's linear-chain structure.

However, certain important differences do exist among the various one-dimensional antiferromagnets. The spin system in TMMC [also in α-CuNSal [α-*bis*(N-methylsalicylaldiminato)-CU(II)] and CuPC ($CuCl_2 \cdot NC_5H_5$) (Refs. 43-45)] is more one-dimensional, to the extent that interchain spin couplings are small enough that they have no significant effect on the collective spin dynamics insofar as the paramagnetic ESR is concerned. But in PCrP-C and CMC, interchain interactions are appreciable and do significantly influence the spin dynamics. In particular, these interactions provide a mechanism for cutting off the slow one-dimensional diffusive decay of dynamic correlations in the torques due to local magnetic and crystalline fields, leading to Lorentzian ESR line shapes for PCrP-C and CMC (also for CTS [$Cu(NH_3)_4\ SO_4 \cdot H_2O$] (Ref. 43)). The line shape for TMMC, on the other hand, is intermediate in character between Lorentzian and Gaussian,[12,19] and the linewidth depends on the local field and exchange strengths in a different way than for

PCrP-C and CMC.

The local fields responsible for the line broadening in both TMMC and CMC are due entirely to the magnetic dipolar interaction. But in PCrP-C the major portion of the ESR linewidth comes from crystal-field site anisotropy, although there is also a smaller contribution from dipolar coupling. Theoretical calculations for a classical spin system show that the effects on the ESR due to intrachain dipolar coupling and site anisotropy can be similar enough to be indistinguishable in experimental observations, particularly with regard to the temperature dependence of the linewidth. Line-shape and linewidth calculations involved in the site anisotropy problem are somewhat simpler than those for the dipolar couplings, since site anisotropy involves only single-spin interactions, rather than multiple-spin, extended range interactions, associated with dipolar coupling. It is worth noting that for quantum spin systems, crystal-field anisotropy and dipolar coupling are expected to have somewhat different effects, since crystal-field anisotropy can be felt only by spins with $s \geq 1$.

PCrP-C is further distinguished by the fact that its chain packing arrangement is disordered, in contrast to the crystalline structure of TMMC and CMC. Three-dimensional spin ordering transitions, induced by exchange-enhanced interchain interactions, occur in both TMMC and CMC at temperatures of 0.84 and 4.89 K, respectively.[46] However, no such transition has been observed in PCrP-C down to a temperature of about 0.02 K, despite the fact that the interchain couplings and intrachain exchange in PCrP-C are comparable in strength to those in CMC. This remarkable difference in behavior is due to the structural disorder in PCrP-C which prevents the coherent enhancement by the intrachain exchange of spin alignments due to the interchain interactions. Such coherent enhancement typically leads to long-range three-dimensional spin ordering. Whereas the one-dimensional magnetic characteristics of TMMC and CMC become obscured near and below their three-dimensional spin ordering temperatures, the spin system in PCrP-C remains fundamentally one-dimensional to much lower temperatures than it would if crystalline order were present. Hence, the structural disorder is distinctly advantageous in this respect, even though there are certain accompanying complications in the data analysis and interpretation.

As strongly suggested by the temperature dependence of the ESR linewidth and the low-temperature susceptibility anisotropy, PCrP-C appears to be further distinguished by inequivalence of the Cr spin sites along the chains. This inequivalence, which manifests itself in terms of variations from site to site in the orientations of the single-site anisotropy axes and in the values of the corresponding principal anisotropy parameters, is associated with the lack of long-range crystalline order and the inequivalence of the three phosphinate bridges between adjacent chromiums due to differences in their organic side groups. The primary effect of this spin-site inequivalence is the suppression of the onset of both the anisotropy spin alignment and the AFMR. Another consequence is the apparent temperature dependence of the effective anisotropy parameter implied by an analysis of the ESR and susceptibility data under the assumption of equivalent spin sites. This result, of course, means that the assumption is incorrect and emphasizes the need for careful interpretation of experiments performed on such systems. Attempts to synthesize chromium-tris-phosphinate polymers with three equivalent bridges have only resulted in mechanically unstable structures resembling brittle crystals. So, at least for the moment, site equivalence seems to necessarily accompany the production of a workable chromium-tris-phosphinate polymer.

The correlation function formalism used to analyze the ESR in PCrP-C is the method that has traditionally been applied to other one-dimensional antiferromagnets like TMMC and CMC.[12,13] While the procedure has, of course, been tailored to accommodate peculiarities of each particular spin system, the quality of the overall agreement between the theory and experiments has so far always been about the same. In particular the temperature dependence of the theoretical ESR linewidth always looks roughly like that shown in Fig. 4, the common features being the asymptotic approach to a constant value at high temperatures and the T^{-3} divergence at low temperatures. Depending on particular interaction parameter values, there may or may not be a minimum in between. These features exist regardless of whether the line broadening mechanism is crystal-field-site anisotropy (with equivalent spin sites) or intrachain magnetic dipolar coupling. The experimental data have displayed the same sort of general behavior, but the observed low-temperature variation has never been quite as strong as T^{-3}, lying in the the range of $T^{-2.0}$ to $T^{-3.0}$, even for systems with equivalent spin sites. There have also been

discrepancies in the intermediate temperature range. While the formal theory does succeed in predicting the correct general type of dynamical behavior for these one-dimensional magnetic systems, it appears that there are inherent inadequacies in the theoretical procedure as evidenced by the persistence of the discrepancies which occur between the theory and experiments. Possible sources for these discrepancies are the neglect in the treatment of the spin-diffusion process of modes with $q \neq 0$, the neglect of spin-correlation effects due to site anisotropy and dipolar coupling, artificial use of simple exponential factors to cut off the low one-dimensional diffusive decay of torque correlations, and quantum effects.

The two-spin, correlated cluster, and random-walk models have proved extremely useful in furnishing a physical understanding of the spin dynamics embodied in the correlation function formalism. The value of these classical models, which correctly reproduce the predictions of the more formal but less transparent theory, lies in their simplicity and their potential for suggesting appropriate modifications to the theory when its inadequacies become apparent. In exploring the effects of the anisotropy alignment at low temperatures, for instance, it might prove more fruitful to first try to develop an extension of the correlated cluster model which accounts for spin correlations due to the site anisotropy in order to obtain at least qualitative predictions of the dynamical behavior of the spin system. The results should then provide an objective framework within which to assess the extent to which the much more complicated formal calculations need to be performed.

ACKNOWLEDGMENTS

This project was funded by the National Science Foundation Grant No. DMR-80-08546 and through the Materials Science Center at Cornell University Grant No. 4520. The authors wish to thank H. D. Gillman for sample preparation.

APPENDIX A: INTERCLUSTER EXCHANGE TORQUES IN THE CORRELATION CLUSTER MODEL

The net exchange torque exerted on sublattice 1 in a correlated spin cluster due to sublattice 2 is given by

$$\vec{\tau}_1 = -2J \sum_{n \text{ odd}} (\vec{s}_{n-1} \times \vec{s}_n + \vec{s}_{n+1} \times \vec{s}_n) . \quad \text{(A1)}$$

Decomposing each $\vec{s}_n$ into its component parallel and perpendicular to its respective sublattice moment yields

$$\vec{\tau}_1 = -2J \sum_{n \text{ odd}} (\vec{s}_{n-1_{\parallel}} \times \vec{s}_{n_{\parallel}} + \vec{s}_{n-1_{\perp}} \times \vec{s}_{n_{\parallel}} + \vec{s}_{n-1_{\parallel}} \times \vec{s}_{n_{\perp}} + \vec{s}_{n-1_{\perp}} \times \vec{s}_{n_{\perp}}$$
$$+ \vec{s}_{n+1_{\parallel}} \times \vec{s}_{n_{\parallel}} + \vec{s}_{n+1_{\perp}} \times \vec{s}_{n_{\parallel}} + \vec{s}_{n+1_{\parallel}} \times \vec{s}_{n_{\perp}} + \vec{s}_{n+1_{\perp}} \times \vec{s}_{n_{\perp}}) . \quad \text{(A2)}$$

The rms magnitudes of these spin components are given by $s_{n_{\parallel}} \simeq s$ and $s_{n_{\perp}} \simeq \theta_1 s$, so the torque expression becomes

$$\vec{\tau}_1 \simeq -2J \sum_{n \text{ odd}} (s^2 \hat{S}_2 \times \hat{S}_1 + s\vec{s}_{n-1_{\perp}} \times \hat{S}_1 + s\hat{S}_2 \times \vec{s}_{n_{\perp}} + \vec{s}_{n-1_{\perp}} \times \vec{s}_{n_{\perp}}$$
$$+ s^2 \hat{S}_2 \times \hat{S}_1 + s\vec{s}_{n+1_{\perp}} \times \hat{S}_1 + s\hat{S}_2 \times \vec{s}_{n_{\perp}} + \vec{s}_{n+1_{\perp}} \times \vec{s}_{n_{\perp}})$$
$$\simeq -2J\xi s^2 \hat{S}_2 \times \hat{S}_1 - 2Js \sum_{n \text{ odd}} (\vec{s}_{n-1_{\perp}} + \vec{s}_{n+1_{\perp}}) \times \hat{S}_1$$
$$- 4Js\hat{S}_2 \times \sum_{n \text{ odd}} \vec{s}_{n_{\perp}} - 2J \sum_{n \text{ odd}} (\vec{s}_{n-1_{\perp}} \times \vec{s}_{n_{\perp}} + \vec{s}_{n+1_{\perp}} \times \vec{s}_{n_{\perp}})$$
$$\simeq -2J\xi s^2 \hat{S}_2 \times \hat{S}_1 - 2J \sum_{n \text{ odd}} (\vec{s}_{n-1_{\perp}} \times \vec{s}_{n_{\perp}} + \vec{s}_{n+1_{\perp}} \times \vec{s}_{n_{\perp}}) , \quad \text{(A3)}$$

where $\hat{S}_1$ are $\hat{S}_2$ are unit vectors along $\vec{S}_1$ and $\vec{S}_2$, and

$$\sum_{n \text{ odd}} \vec{s}_{n_{\perp}} = \sum_{n \text{ odd}} \vec{s}_{n_{\perp}} = 0 .$$

The corresponding torque on sublattice 2 due to sublattice 1 is simply $\vec{\tau}_2 = -\vec{\tau}_1$.

The first term has a magnitude of

$$\sim 2 |J| \xi s^2 \gamma \sim |J| s^2 ,$$

since

$$|\hat{S}_2 \times \hat{S}_1| = \sin\gamma \sim \gamma \, .$$

This term gives rise to a precession of $\vec{S}_1$ and $\vec{S}_2$ about $\vec{S}$ as in the two-spin model. The magnitude of the second term is

$$\sim 2|J|\xi^{1/2}\theta_1^2 s^2 \sim (T/T_e)^{1/2}|J|s^2 \, ,$$

since the contributions from the various pairs of spins add incoherently because $\vec{s}_{n_\perp}$ is thermally excited. This term will be neglected compared to the first since $T << T_e$. At most its effect would be simply to introduce some jerkiness into the precession of $\vec{S}_1$ and $\vec{S}_2$ about $\vec{S}$, since internal cluster torques cannot alter $\vec{S}$. Hence, τ_1 and τ_2 are both $\sim |J| s^2$.

APPENDIX B: INTERCHAIN DIPOLAR COUPLING IN THE RANDOM-WALK MODEL

Consider an array of parallel chains with equally spaced sites occupied by identical mobile spins. Let t_e and t_c be the mean intrachain and interchain spin hopping times, respectively. During a time $t >> t_e$, spins diffuse along their respective chains over a distance of the order of the diffusion length $r(t) \sim (t/t_e)^{1/2}$. If the interchain hopping is attributed to magnetic dipolar coupling, then t_c actually characterizes the correlation time for the orientation of any one spin. Hence, the contribution to the precessional phase acquired by any particular spin due to its interaction with any other particular spin accumulates coherently with time over a time scale $t \lesssim t_c$. However, at high temperatures where the distribution of spin orientations is random, contributions to any one spin's precessional phase due to interactions with different spins add incoherently.

After a time t ($>> t_e$, but $<< t_c$), the phase $\phi_{nm}(t)$ acquired by a spin initially at site n on chain 1 due to the dipolar torque exerted on it by a spin initially at site m on neighboring chain 2 is the product of t and the average torque exerted in that time, namely

$$\phi_{nm}(t) \sim g^2\mu_B^2 s(s+1)\left[\sum_{n'}^{n\pm r(t)}\sum_{m'}^{m\pm r(t)} f(n'm')r_{n'm'}^{-3} \Big/ [2r(t)]^2\right] t$$

$$\sim g^2\mu_B^2 s(s+1)\sum_{n'}^{n\pm r(t)}\sum_{m'}^{m\pm r(t)} f(n'm')r_{n'm'}^{-3} t_e \, , \tag{B1}$$

where the large parenthesis enclose the angular and distance factors, $f(n'm')$ and $r_{n'm'}^{-3}$, averaged over all sites n' and m' within roughly a diffusion length of the initial sites n and m. The net phase $\phi_n(t)$ acquired by the spin on chain 1 due to all the spins on chain 2 is the incoherent unrestricted sum over m of $\phi_{nm}(t)$, namely

$$\phi_n(t) \sim \left[\sum_m^{\text{all}} \phi_{nm}^2(t)\right]^{1/2}$$

$$\sim g^2\mu_B^2 s(s+1)\left[\sum_m^{\text{all}}\sum_{n'}^{n\pm r(t)}\sum_{m'}^{n\pm r(t)}\sum_{n''}^{n\pm r(t)}\sum_{m''}^{n\pm r(t)} f(n'm')f(n''m'')r_{n'm'}^{-3}r_{n''m''}^{-3}\right]^{1/2} t_e \, . \tag{B2}$$

The summations may be simplified as follows. If $r(t) >> 1$ and $|n-m| << r(t)$, then

$$\sum_{n'}^{n\pm r(t)}\sum_{m'}^{n\pm r(t)} f(n'm')r_{n'm'}^{-3} \sim \sum_{n'}^{n\pm r(t)}\sum_{m'}^{\text{all}} f(n'm')r_{n'm'}^{-3} \sim r(t)\sum_{m'}^{\text{all}} f(Om')r_{Om'}^{-3} \, ,$$

where the restricted sum over m' can be extended to an unrestricted sum because of the convergence factor $r_{n'm'}^{-3}$, and the sum over n' then consists of roughly $r(t)$ identical terms. Similarly for the sums over n'' and m''. If, however, $|n-m| >> r(t)$, then the contribution of these sums to the total is insignificant, again because of the convergence factors. Hence, the sum over m also reduces to roughly $r(t)$ identical terms. Therefore,

$$\phi_n(t) \sim g^2\mu_B^2 s(s+1)\left[r^3(t)\sum_{m'}^{\text{all}} f(Om')r_{Om'}^{-3}\sum_{m''}^{\text{all}} f(Om'')r_{Om''}^{-3}\right]^{1/2} t_e \sim g^2\mu_B^2 s(s+1)\sum_{m'}^{\text{all}} f(Om')r_{Om'}^{-3} t_e^{1/4} t^{3/4} \, . \tag{B3}$$

If the effects of all neighboring chains had been included, this expression would become

$$\phi_n(t) \sim J_d t_e^{1/4} t^{3/4} , \tag{B4}$$

where

$$J_d = \left[\sum_{\text{chains}} J_{d\ \text{chains}}^2 \right]^{1/2}$$

and

$$J_{d\ \text{chain}} = g^2 \mu_B^2 s(s+1) \sum_{m'}^{\text{all}} f(Om') r_{Om'}^{-3} . \tag{B5}$$

The interchain hopping time t_c is defined by setting $\phi_n(t_c) \sim 1$, which gives

$$\frac{1}{t_c} \sim J_d^{4/3} t_e^{1/3} \tag{B6}$$

as indicated in Sec. IV.

[1]R. E. Stahlbush, C. M. Bastuscheck, A. K. Raychaudhuri, J. C. Scott, D. Grubb, and H. D. Gillman, Phys. Rev. B 23, 3393 (1981); R. E. Stahlbush, Ph.D. thesis, Cornell University, 1980 (unpublished).

[2]P. D. Krasicky, J. C. Scott, R. H. Silsbee, and A. L. Ritter, J. Phys. Chem. Solids 39, 991 (1978).

[3]K. W. H. Stevens, in *Magnetism,* edited by G. T. Rado and H. Suhl (Academic, New York, 1963), Vol. 1, p. 1.

[4]B. Bleaney and K. W. H. Stevens, *Reports on Progress in Physics* (Physical Society, London, 1953), Vol. 16, p. 108.

[5]K. D. Bowers and J. Owen, *Reports on Progress in Physics* (Physical Sociey, London, 1955), Vol. 18, p. 3.

[6]S. A. Al'tschuler and B. M. Kozyrev, *Electron Paramagnetic Resonance* (Academic, New York, 1964).

[7]J. W. Orton, *Electron Paramagnetic Resonance* (Illife, London, 1968).

[8]G. E. Pake, *Paramagnetic Resonance,* 1st ed. (Benjamin, New York, 1962).

[9]G. E. Pake and T. L. Estle, *The Physical Properties of Electron Paramagnetic Resonance,* 2nd ed. (Benjamin, Reading, Massachusetts, 1973).

[10]C. P. Slichter, *Principles of Nuclear Resonance* (Springer, New York, 1978).

[11]A. Abragam, *The Principles of Nuclear Magnetism* (Oxford University Press, London, 1961).

[12]T. T. P. Cheung, Z. G. Soos, R. E. Dietz, and F. R. Merritt, Phys. Rev. B 17, 1266 (1978).

[13]Y. Tazuke and K. Nagata, J. Phys. Soc. Jpn. 38, 1003 (1975).

[14]P. D. Krasicky, Ph.D. thesis, Cornell University, 1980 (unpublished).

[15]L. R. Walker, in *Magnetism,* edited by G. T. Rado and H. Suhl (Academic, New York, 1963), Vol. 1, p. 299.

[16]R. Kubo, Phys. Rev. 87, 568 (1952).

[17]P. W. Anderson, Phys. Rev. 86, 694 (1952).

[18]M. Steiner, J. Villain, and C. G. Windsor, Adv. Phys. 25, 87 (1976).

[19]P. M. Richards, in *Low Dimensional Cooperative Phenomena,* edited by H. J. Keller (Plenum, New York, 1975), p. 147.

[20]P. W. Anderson and P. R. Weiss, Rev. Mod. Phys. 25, 269 (1953).

[21]N. Bloombergen, E. M. Purcell, and R. V. Pound, Phys. Rev. 73, 679 (1948).

[22]M. N. Barber and B. W. Ninham, *Random and Restricted Walks* (Gordon and Breach, New York, 1970).

[23]J. Owen, J. Appl. Phys. 32, 2135 (1961).

[24]S. Foner, in *Magnetism,* edited by G. T. Rado and H. Suhl (Academic, New York, 1963), Vol. 1, p. 383.

[25]F. Keffer and C. Kittel, Phys. Rev. 85, 329 (1952).

[26]M. E. Fisher, Am. J. Phys. 32, 343 (1964).

[27]J. M. Loveluck, S. W. Lovesey, and S. Aubrey, J. Phys. C 8, 3841 (1975); J. M. Loveluck, and S. W. Lovesey, *ibid.* 8, 3857 (1975).

[28]G. F. Reiter and J. P. Boucher, Phys. Rev. B 11, 1823 (1975).

[29]F. Lado, J. D. Memory, and G. W. Parker, Phys. Rev. B 4, 1406 (1971).

[30]G. Reiter and F. C. Barreto, Phys. Rev. B 8, 1935 (1973).

[31]H. Mori, Prog. Theor. Phys. 33, 423 (1965).

[32]J. H. Van Vleck, Phys. Rev. 74, 1168 (1948).

[33]H. Mori and K. Kawasaki, Prog. Theor, Phys. 27, 529 (1962).

[34]N. A. Lurie, D. L. Huber, and M. Blume, Phys. Rev. B 9, 2171 (1974).

[35]F. B. McLean and M. Blume, Phys. Rev. B 7, 1149 (1973).

[36]L. S. Singer, J. Chem. Phys. 32, 379 (1975).

[37]S. Sugano and R. G. Shulman, Phys. Rev. 130, 517 (1963).

[38]R. G. Shulman and S. Sugano, Phys. Rev. 7, 157 (1961).

[39]A. J. Freeman and R. E. Watson, Phys. Rev. 120, 1254 (1960).

[40]D. E. Rimmer, *Proceedings of the International Conference on Magnetism, Nottingham, 1964* (Institute of Physics and Physical Society, London, 1964), p. 337.

[41]R. E. Stahlbush and J. C. Scott, Solid State Commun.

33, 707 (1980).
[42]J. des Cloizeaux and J. J. Pearson, Phys. Rev. 128, 2131 (1962).
[43]M. J. Hennessy, C. D. McElwee, and P. M. Richards, Phys. Rev. B 7, 930 (1973)
[44]R. R. Bartkowski, M. J. Hennessy, B. Morosin, and P. M. Richards, Solid State Commun. 11, 405 (1972).
[45]R. R. Bartkowski and B. Morosin, Phys. Rev. B 6, 4209 (1972).
[46]K. Nagata and Y. Tazuke, J. Phys. Soc. Jpn. 32, 337 (1972).